

# Bridging AI and BNP for Layered Point Pattern Data Analysis

NSF-ICERM  
BNP Inference - Computational Issues

Qiwei Li  
Associate Professor of Statistics

Department of Mathematical Sciences  
The University of Texas at Dallas



# Table of Contents

**1** Background

**2** AI-derived Data

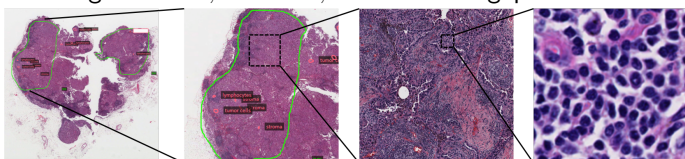
**3** Statistical Inference

**4** Results

**5** Summary

# Tumor Pathology Images

- Capture histological details in high resolution
  - Average size:  $25,000 \times 20,000 = 500$  megapixels



- Require a systematical exploration on subtle patterns
- Harbor a large amount of biological information

- Cell growth pattern
  - Survival outcome (Gleason *et al.*, 2002; Amin *et al.*, 2002; Borczuk *et al.*, 2009; Barletta *et al.*, 2010)
  - Treatment response (Tsao *et al.*, 2015)
- Cell-cell interaction
- Cell interaction with the surrounding micro-environment

AI-Statistics for Pathology Image Analysis

- AI discovers complex patterns, but lacks interpretability

## AI-Statistics for Pathology Image Analysis

- AI discovers complex patterns, but lacks interpretability
- Statistics interprets data, but cannot afford complex data

AI-Statistics for Pathology Image Analysis

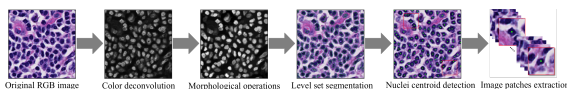
- AI discovers complex patterns, but lacks interpretability
- Statistics interprets data, but cannot afford complex data
- AI-Statistics workflow



## AI - ConvPath Pipeline

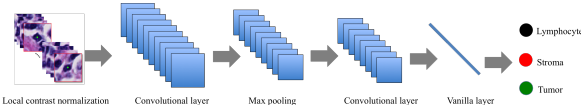
## ■ Cell segmentation with water-shed method

- Yi et al., Automatic extraction of cell nuclei from H&E-stained histopathological images (2017), *J. Med. Imaging*, **4**(2)

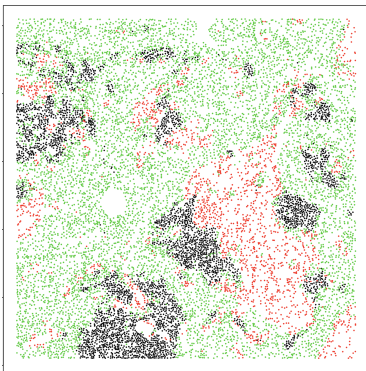
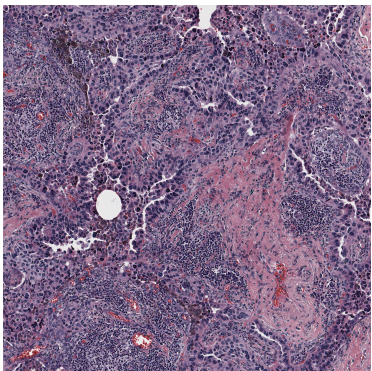


## ■ Cell type classification by deep learning

- Wang *et al.*, ConvPath: A software tool for lung adenocarcinoma digital pathological image analysis aided by a convolutional neural network (2019), *EBioMedicine*, **50**

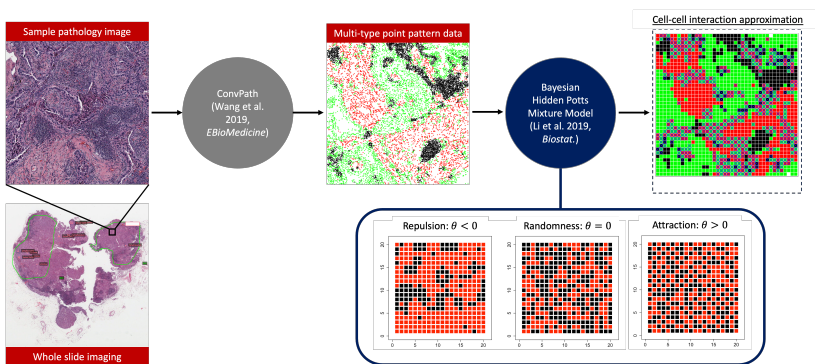


## Data - Multi-type Point Patterns

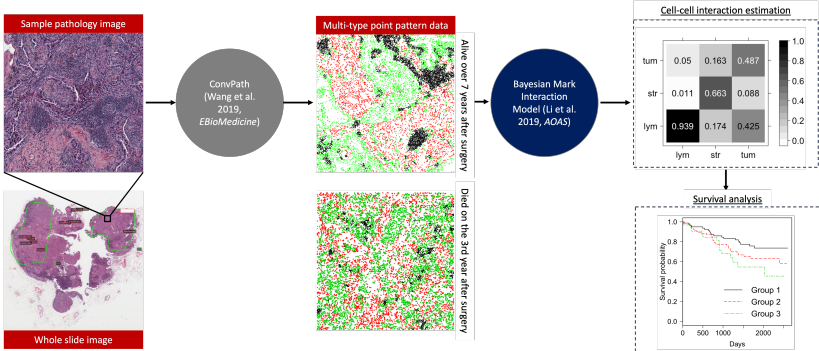


- Raw data: pathology images
- Processed data: multi-type point pattern data
  - Locations:  $(x_i, y_i), i = 1, \dots, n$
  - Marks:  $z_i \in \{\text{Lymphocyte} (\bullet), \text{stromal} (\bullet), \text{and tumor} (\bullet)\}$

AI-Bayesian for Point Pattern Data Analysis



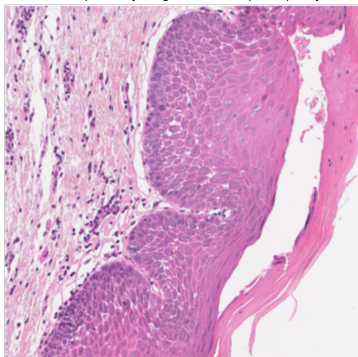
# AI-Bayesian for Point Pattern Data Analysis



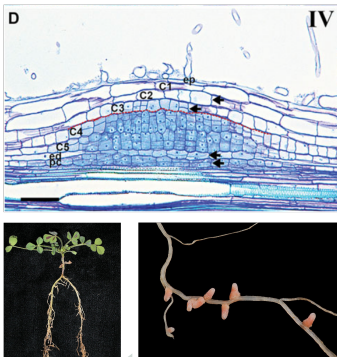
# Motivation

- Motivation: the number of epithelial layers is linked to dysplasia severity in oral cancer
- Goal: estimate the number of cellular layers in an image

A cropped WSI from a patient in the oral potentially malignant disorders (OPMD) study

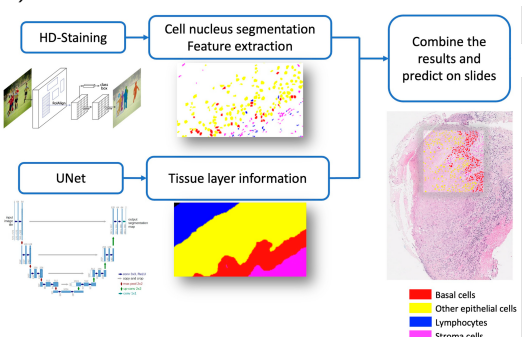


A micrograph image slide from *medicago truncatula* root nodule

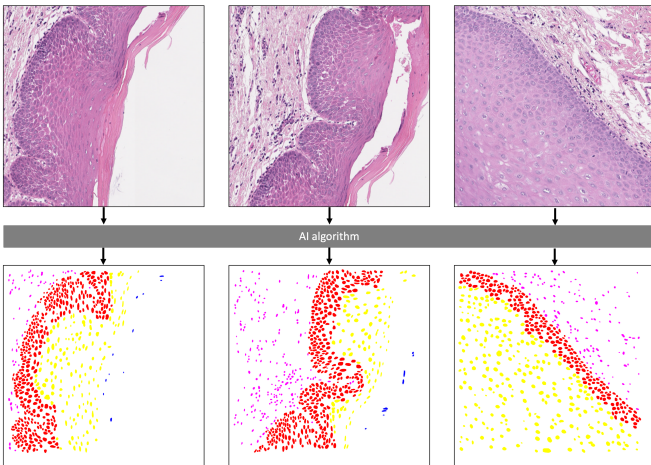


# AI - Deep Convolutional Neural Network

- Cell nuclei segmentation and classification using HD-staining (Wang *et al.*, *Cancer Res.*, 2020) and YOLOv8 mask (Rong *et al.*, *Mod. Pathol.*, 2023)
- Tissue layer segmentation using U-Net (Ronneberger *et al.*, *MICCAI'15*)



# Data - Multi-type Point Patterns

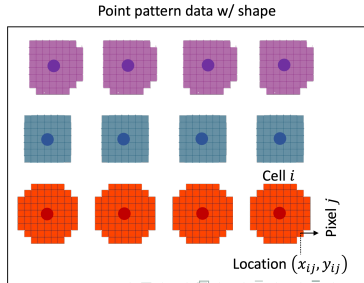
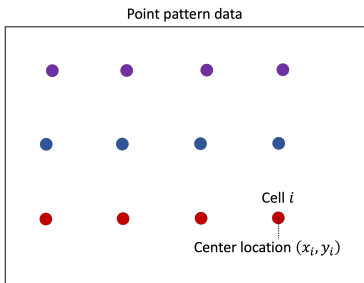


# Data - Multi-type Point Patterns

- Raw data: oral tissue pathology images
  - 128 oral potentially malignant disorders (OPMD) patients from the Erlotinib Prevention of Oral Cancer (EPOC) trial at UT MDACC
  - 701 sample images (in 4 megapixels) from 255 whole slide images (WSI)
- Processed data: multi-type point pattern data
  - The number of cells  $n$  ranges from 169 to 3,003
  - Locations:  $(x_i, y_i), i = 1, \dots, n$
  - Marks:  $z_i \in \{\text{Lymphocytes} (\bullet), \text{stroma cells} (\bullet), \text{and epithelial cells} (\bullet \text{ and } \bullet)\}$

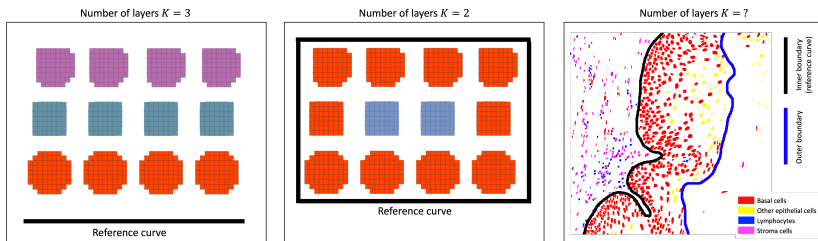
# Data - Point Patterns w/ Shape

- Processed data: point pattern data w/ shape
  - Locations of cell nuclei:  $(x_i, y_i), i = 1, \dots, n$
  - Marks:  $z_i \in \{\text{Lymphocytes} (\bullet), \text{stroma cells} (\bullet), \text{and epithelial cells} (\bullet \text{ and } \bullet)\}$
  - Cell nucleus pixel:  $(x_{ij}, y_{ij}), i = 1, \dots, n$  and  $j = 1, \dots, m_i$ , where  $m_i$  is the number of total pixels in cell nucleus  $i$



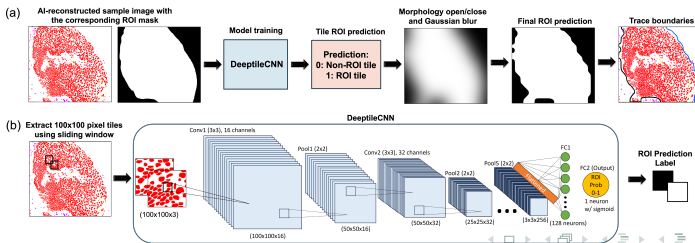
# Data - Reference Curves

- Layered structure depends on the selection of reference curves
- Pathologists define the outer boundary near the corneum cells (layers are less distinct), and the inner boundary near the denser stromal regions



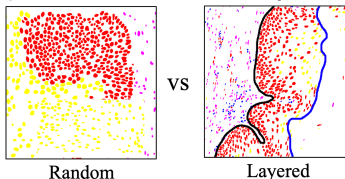
# AI - DeeptileCNN

- Boundary detection is approached as tile classification
- Region of interest (ROI) classification using DeeptileCNN
  - Tiles were labeled as ROI if  $\geq 75\%$  of pixels overlapped with the ground-truth ROI mask
  - Size: 55,613 (training), 15,930 (validation), and 7965 (test)
  - Overall accuracy: 87.1% (training) and 85.5% (test)
  - Gaussian smoothing was used to reduce blocky edges by tiling

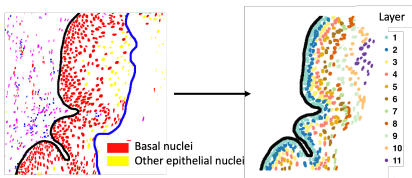


# Research Goals

- To study the layered structure in point pattern data
  - To test if point pattern data exhibit a layered structure

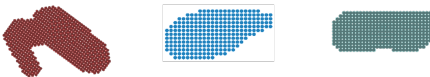


- To estimate the number of layers from layered point pattern data

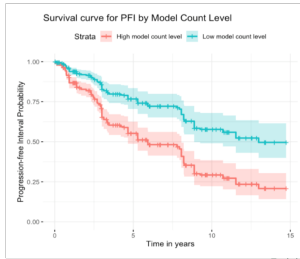


# Research Goals

- To characterize shape of cell nuclei

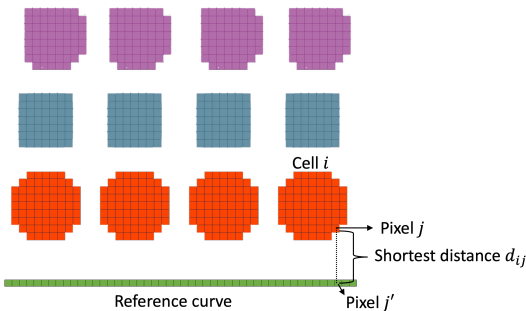


- To assess the clinical significance of epithelial layer numbers and oral cancer progression

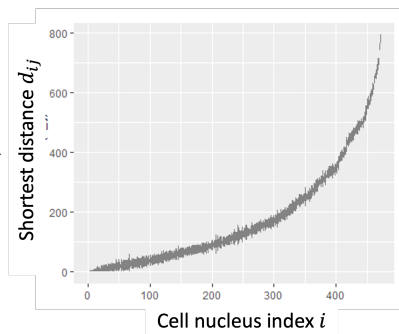
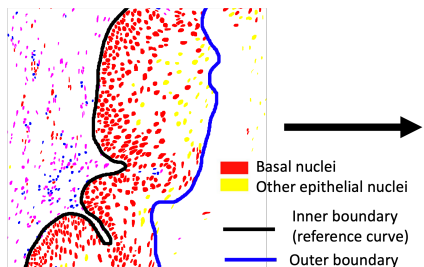


# BLADE - Input Data

- Input data  $d_{ij}$ : the shortest Euclidean distance from the pixel  $j$  in cell nucleus  $i$  to the reference curve
- $\mathbf{d}_{i\cdot} = (d_{i1}, \dots, d_{i,m_i})$  captures the spatial position of each cell nucleus  $i$  to the reference curve

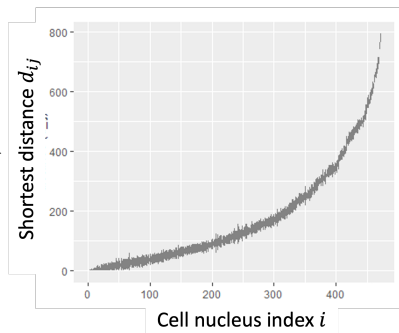
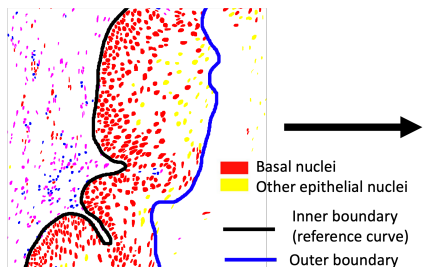


# BLADE - Input Data



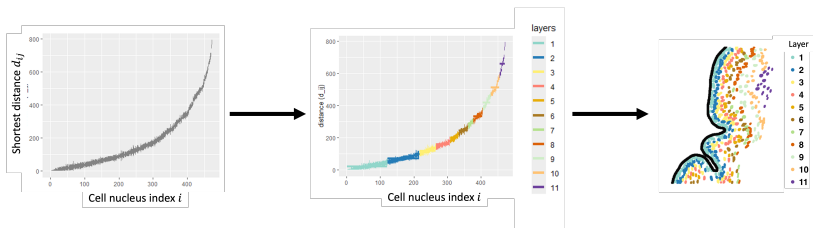
- Each bar represents a cell nucleus  $i$
- The two ends of each bar  $i$  indicating the range of shortest distances  $\mathbf{d}_{i\cdot} = (d_{i1}, \dots, d_{im_i})$

# BLADE - Input Data



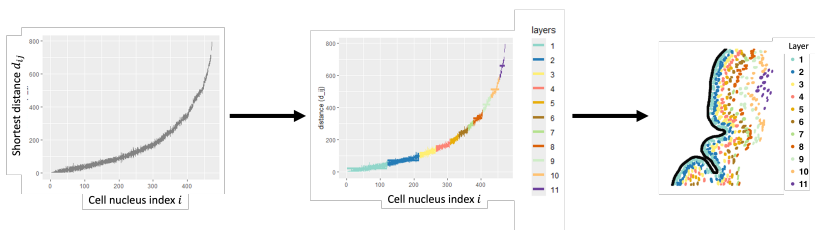
- Each bar represents a cell nucleus  $i$
- The two ends of each bar  $i$  indicating the range of shortest distances  $\mathbf{d}_{i\cdot} = (d_{i1}, \dots, d_{im_i})$
- View  $\mathbf{d}_{i\cdot}$  as sampling points from a function

# BLADE - Overview



- Cluster the functions with sampling points  $d_{i\cdot}, i = 1, \dots, n$  into distinct groups in a sequential order
  - Not necessary to include all elements in  $d_{i\cdot}$  to reconstruct the nucleus shape

# BLADE - Overview



- Cluster the functions with sampling points  $d_{i\cdot}, i = 1, \dots, n$  into distinct groups in a sequential order
  - Not necessary to include all elements in  $d_{i\cdot}$  to reconstruct the nucleus shape
- What is the most appropriate function?
- What is the most appropriate clustering approach?

# BLADE - Shape Component

- Assume  $d_{ij}$  follows a generalized Beta (GBe) distribution:

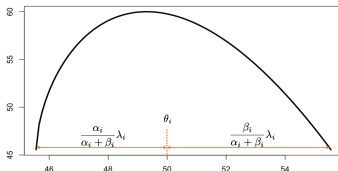
$$d_{ij} | \alpha_i, \beta_i, \theta_i, \lambda_i \sim \text{GBe}(\alpha_i, \beta_i, \theta_i, \lambda_i)$$

- p.d.f.:  $f(d_{ij} | \alpha_i, \beta_i, \theta_i, \lambda_i) =$

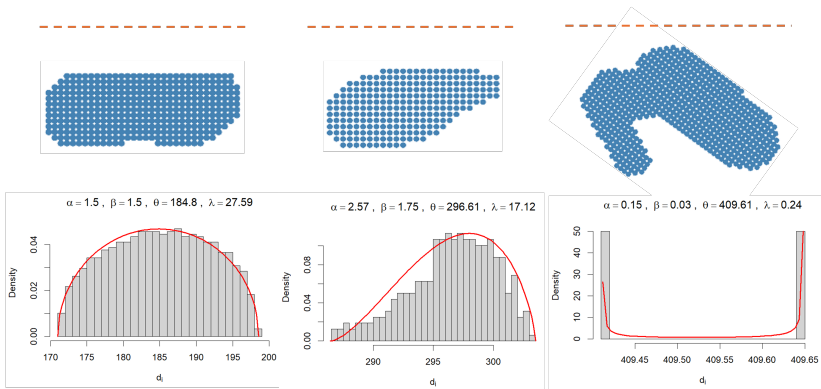
$$\frac{\Gamma(\alpha_i + \beta_i)}{\Gamma(\alpha_i)\Gamma(\beta_i)} \frac{\left(d_{ij} - \theta_i + \frac{\alpha_i}{\alpha_i + \beta_i} \lambda_i\right)^{\alpha_i - 1} \left(-d_{ij} + \theta_i + \frac{\alpha_i}{\alpha_i + \beta_i} \lambda_i\right)^{\beta_i - 1}}{\lambda_i^{\alpha_i + \beta_i - 2}}$$

- Relationship with the Beta distribution:

$$\frac{d_{ij} - \left(\theta_i - \frac{\alpha_i}{\alpha_i + \beta_i} \lambda_i\right)}{\lambda_i} \sim \text{Beta}(\alpha_i, \beta_i)$$

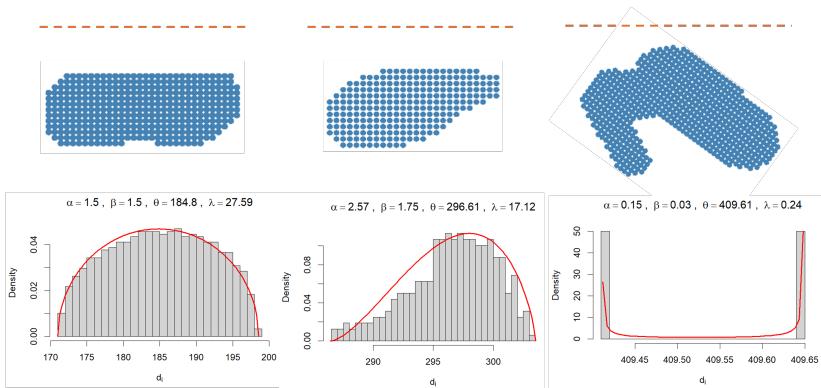


# BLADE - Shape Component



- The estimated shape parameters  $\alpha_i$  and  $\beta_i$  for three representative cell nuclei

# BLADE - Shape Component



- The estimated shape parameters  $\alpha_i$  and  $\beta_i$  for three representative cell nuclei
- Extended to  $\alpha_k$  and  $\beta_k$ , assuming nuclei shape is similar

# BLADE - FMM

- Adjust for the shape effect *via* the GBe model
- The stratification focuses on clustering the mean shortest distances  $\theta_i$ 's

# BLADE - FMM

- Adjust for the shape effect *via* the GBe model
- The stratification focuses on clustering the mean shortest distances  $\theta_i$ 's
- Let  $z = (z_1, \dots, z_n)$  denote the latent layers, where  $z_i = k$  indicates the cell nucleus  $i$  belongs to layer  $k$
- GMM with conjugate prior

$$\theta_i | z_i = k, \mu_k, \sigma_k^2 \sim N(\mu_k, \sigma_k^2)$$

$$\mu_k, \sigma_k^2 \sim NIG(\mu_0, p_0, \nu_0/2, SS_0/2)$$

$$z_i | \omega \sim Multi(1, \omega), \omega \sim Dir(\gamma)$$

# BLADE - DPMM

- In the Dirichlet process (DP), the weight  $\omega_k$  is constructed *via* stick-breaking process:

$$\omega_k = v_k \prod_{h=1}^{k-1} (1 - v_h), \quad v_k \sim \text{Be}(1, \gamma)$$

- $\gamma$  is the concentration parameter that controls the variation of the DP prior around its mean  $G_0$

- DPMM

$$\theta_i | \mu_i, \sigma_i^2 \sim \mathcal{N}(\mu_i, \sigma_i^2)$$

$$\mu_i, \sigma_i^2 | G \sim G$$

$$G \sim \text{DP}(G_0, \gamma), \text{ where } G_0 = \text{NIG}(\mu_0, p_0, \nu_0/2, SS_0/2)$$

# BLADE - DPMM

- The random partition can be generated with an urn scheme or a Chinese restaurant process (CRP)
  - The conditional distribution for each  $z_i$  is:

$$\Pr(z_i = k \mid \mathbf{z}_{-i}) \propto \begin{cases} n_{k,-i} & \text{for an existing cluster} \\ \gamma & \text{if } c \text{ is a new cluster} \end{cases},$$

- As the sample size grows,  $\hat{K}$  remains inconsistent due to the presence of extraneous clusters in the posterior
- Flexible but often leads to overestimation of clusters.

# BLADE - MFM

- Mixture of Finite Mixtures (MFM) proposed by Miller and Harrison (*JASA*, 2018)

$$z_i|K, \pi \sim \sum_{k=1}^K \pi_k I(z_i = k), \quad \pi|K \sim \text{Dir}(\gamma), \quad K-1 \sim \text{Poi}(\tau)$$

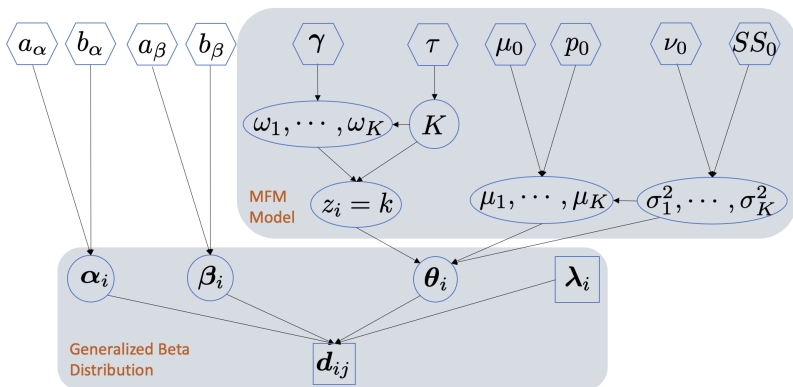
- The conditional distribution for each  $z_i$  under MFM is:

$$\Pr(z_i = k \mid \mathbf{z}_{-i}) \propto \begin{cases} n_{k,-i} + \gamma & \text{for an existing cluster } k \\ \frac{V_n(|\mathbf{z}_{-i}|+1)}{V_n(|\mathbf{z}_{-i}|)} \gamma & \text{if } k \text{ is a new cluster} \end{cases}$$

- Reduces the likelihood of forming extraneous clusters as  $\frac{V_n(|\cdot|+1)}{V_n(|\cdot|)} < 1$
- Avoids overestimation as number of clusters converges to a finite value

# BLADE - Wrap-up

## ■ Graphical representation:

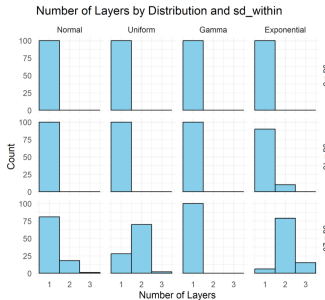


# BLADE - Hypothesis Testing

- To test whether a given point pattern exhibits a layered structure or not *via* Bayes factor (BF)

$$BF = \frac{\Pr(K = 1|\cdot) / \Pr(K \geq 2|\cdot)}{\Pr(K = 1) / \Pr(K \geq 2)} = \frac{\sum_{t=1}^T I(|\mathbf{z}^{(t)}| = 1) / I(|\mathbf{z}^{(t)}| \geq 2)}{e^{-\tau} / (1 - e^{-\tau})}$$

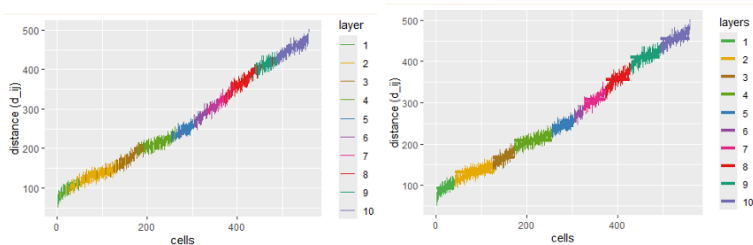
- When MFM prior assumes  $K - 1 \sim \text{Poi}(\tau)$



# BLADE - Simulation

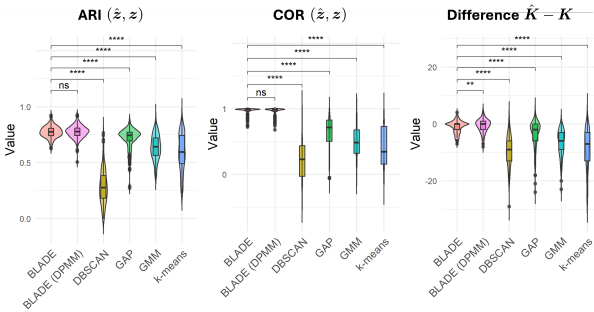
## ■ Simulation setup:

- Generated 200 simulated datasets
- $K_{\text{true}} \sim U(5, 35)$ ,  $n_k \sim N_{[20,200]}(100, 60^2)$ , and  $m_i \sim U(90, 150)$



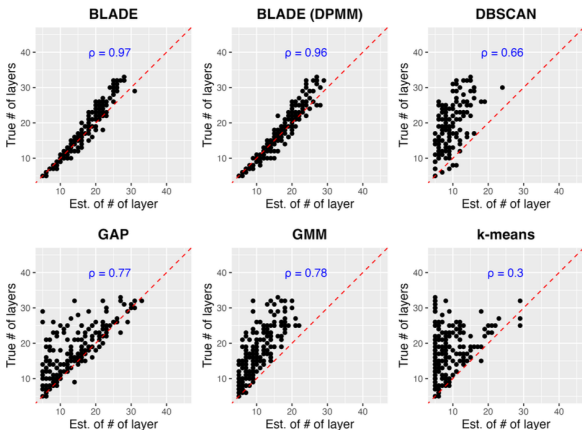
# BLADE - Simulation

- Comparison of layered structures estimated by BLADE and other methods



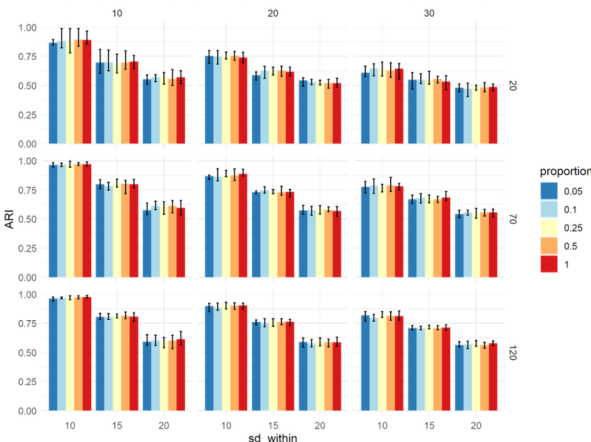
# BLADE - Simulation

- Comparison of layered structures estimated by BLADE and other methods



# BLADE - Simulation

- BLADE maintained high ARI scores even when only a small proportion of pixel-level data  $d_{ij}$  were used.

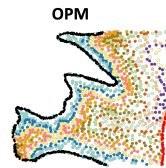
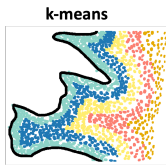
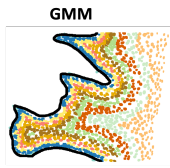
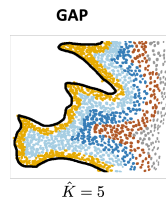
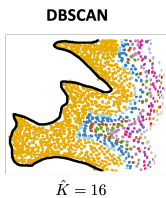
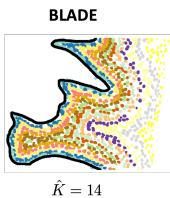


# BLADE - Oral Tissue Pathology Images

- Oral cancer is the sixth most common cancer globally
- Early detection increases survival: 83.7% (early) vs. 38.5% (late stage)
- 128 patients with oral potentially malignant disorders (OPMD) from the erlotinib prevention of oral cancer (EPOC) trial at UT MDACC
- Clinical Data:
  - Demographics: age, gender
  - Risk factors: prior/concurrent oral cancer, TP53 mutation, LOH eligibility, leukoplakia group, HistBaselineR3
  - Outcomes: progression-free interval (PFI) status and time: 1 = progression observed and 0 otherwise

# BLADE - Oral Tissue Pathology Images

- The layered structures estimated by BLADE and the other methods for patient 076



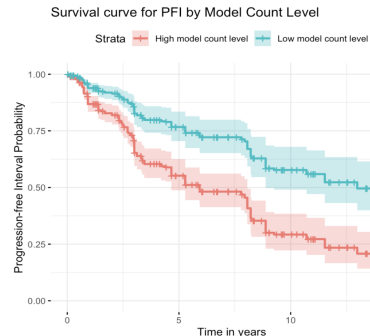
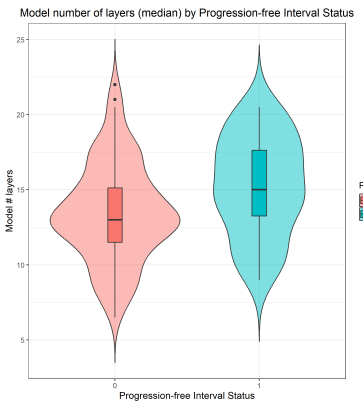
# BLADE - Oral Tissue Pathology Images

- Model-derived layer count is significantly associated with disease progression
- Each additional layer increases the risk of progression by approximately 8%

Variable	Coefficient	Exp(Coef.)	SE	Pr(> z )
$\hat{K}$ by BLADE	0.0771	<b>1.0801</b>	0.0237	<b>0.00113</b>
Age	-0.0302	0.9703	0.0156	0.05370
Male vs. female	-0.4778	0.6201	0.4149	0.24945
Prior oral cancer	0.9873	2.6841	0.3854	<b>0.01042</b>
Concurrent oral cancer	0.7515	2.1203	0.6273	0.23091
Leukoplakia group	0.4116	1.5092	0.6335	0.51589
LOH Eligible	0.4665	1.5944	0.3864	0.22727

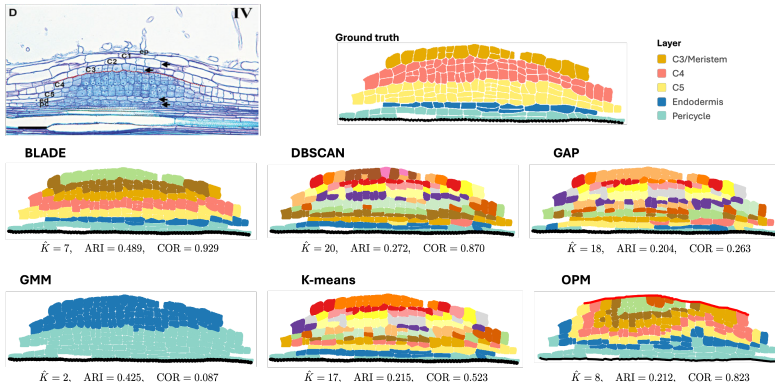
# BLADE - Oral Tissue Pathology Images

- Patients with PFI status = 1 exhibited higher median layer counts compared to those with PFI status = 0



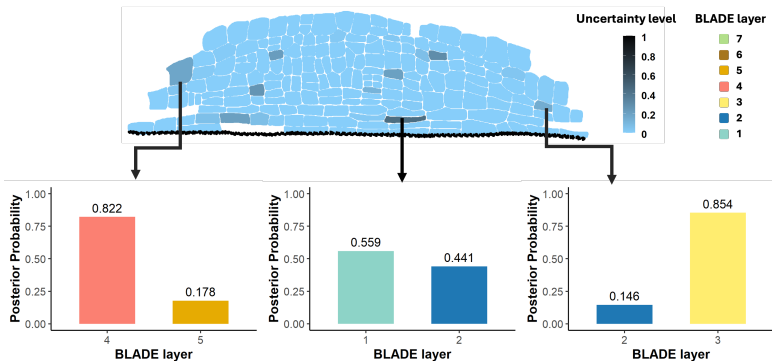
# BLADE - *Medicago Truncatula* Root Nodule

- The layered structures at STAGE IV estimated by BLADE and the other methods



# BLADE - *Medicago Truncatula* Root Nodule

- BLADE can also quantify the uncertainty, which can be defined as the posterior probability  $\Pr(z_i \neq \hat{z}_i | \cdot)$



# Summary

- Statistical shape and spatial analysis under the AI-Statistics workflow



- Bayesian nonparametric model for analyzed layered point pattern data
  - Test if point pattern data exhibit a layered structure
  - Estimate the number of layers from point pattern data
  - Effectively characterize cell nucleus shape information

The End

Thanks for your attention!

## ■ Acknowledgment



DMS-2210912  
DMS-2113674



1R01GM141519  
1R01DK131267